Corrected electrostatic model for dipoles adsorbed on a metal surface

Brian L. Maschhoff, and James P. Cowin

Citation: The Journal of Chemical Physics **101**, 8138 (1994); doi: 10.1063/1.468241
View online: https://doi.org/10.1063/1.468241
View Table of Contents: http://aip.scitation.org/toc/jcp/101/9
Published by the American Institute of Physics

Corrected electrostatic model for dipoles adsorbed on a metal surface

Brian L. Maschhoff and James P. Cowin
Enviornmental and Molecular Science Laboratory, Pacific Northwest Laboratories[a] *Box 999 MS K2-14, Richland, Washington 99352*

(Received 10 February 1994; accepted 11 July 1994)

We present a dipole–dipole interaction model for polar molecules vertically adsorbed on a idealized metal surface in an approximate analytic form suitable for estimating the coverage dependence of the work function, binding energies, and thermal desorption activation energies. In contrast to previous treatments, we have included all contributions to the interaction energy within the dipole model, such as the internal polarization energy and the coverage dependence of the self-image interaction with the metal. We show that these can contribute significantly to the total interaction energy. We present formulae for both point and extended dipole cases.

I. INTRODUCTION

Evidence for lateral interactions between molecules adsorbed on metal surfaces is available from a number of experiments.[1–11] In some cases the lateral interactions have been ascribed primarily to simple electrostatic dipole-dipole interactions. In temperature programmed desorption (TPD) experiments, strongly decreasing desorption activation energies with coverage are observed for alkali atoms and a number of polar adsorbates.[1–5] Induced dipole–dipole interactions in adsorption of rare gases are closely related, and well studied.[6] For the molecular systems, an orientation specific chemical interaction between one end of the molecule and the surface favors a overlayer structure (at or below one monolayer) with all dipoles pointing in the same direction. This causes a mutual destabilization. Conversely, stabilizing effects due to coadsorption have also been observed. Cooperative ordering of carbon monoxide and benzene on several metal surfaces has been ascribed to dipole interactions.[8] Such interactions are also important in describing coverage dependent surface dynamics, as in the vibrational frequencies for dipolar adsorbates.[9–11]

Several authors have developed very simple classical electrostatic models which can qualitatively account for the coverage dependent observations in simple forms easily applicable to experimental thermal desorption, isotherms, and work function measurements. These papers are important in that they allow experimentalists to easily estimate the effects of dipole–dipole interactions. The adsorbates are typically treated as a point dipoles, with a scalar polarizability, located a fixed distance above an ideal metal (with infinite polarizability). Analytic expressions for the interactions developed originally for modeling surface work function changes,[12–15] have more recently been used for adsorbate dipole inter-repulsions.[3,4]

However, there are two aspects of these simple treatments which are in error. First, two contributions to the total electrostatic interaction between dipoles near a metal surface, specifically dipole internal polarization energy and changes in the dipole self-image interaction, have commonly been neglected. We will show in this paper that these are quantitatively significant contributions. Second, the relationship between the electrostatic potential energy per dipole (a thermodynamic quantity) and the resultant change in the desorption activation energy has often been interpreted incorrectly. These topics are discussed further below.

Any real adsorbate, with or without a permanent dipole moment μ_0, will be polarizable, meaning that an external electric field will induce a change μ_{ind} in the dipole such that $\mu=\mu_0+\mu_{\text{ind}}$. For dipoles aligned on a surface, μ at coverages approaching saturation can be considerably less than μ_0. For example, inclusion of polarizability is crucial in predicting work function changes at high coverages.[13] As a result of polarization, the internal energy of the dipole increases by $(1/2)\mu_{\text{ind}}\cdot E$; this represents work performed by the electric field on the dipole.[16–18] This contribution to the potential energy of the dipole has been neglected in several previous simple treatments.

Many treatments have assumed that the total binding energy is given by the sum of a coverage dependent interaction energy and a constant energy term, the latter being determined at the low coverage limit. However, part of the molecule/surface binding energy is due to the electrostatic attraction of the dipole to its classical image in the metal, which we term the self-image energy. As the coverage is increased, and each molecule is depolarized by the surrounding electric field, this self-image energy decreases in magnitude. Thus the overall effect is a further destabilization of the binding of each dipole to the surface. Therefore, the dipole interaction energy must include this self-image energy change explicitly.

Finally, there is some confusion in this literature as to how to estimate the coverage dependence of thermal desorption. For thermal desorption kinetics the most relevant quantity is the negative of the differential energy of adsorption, essentially the energy to removal of a single molecule, not the average binding energy per molecule. In several simple treatments, however, the dipole effects on the desorption activation energy has been equated to the negative product of

[a]Pacific Northwest Laboratory is a multiprogram national laboratory operated by Battelle Memorial Institute for the Department of Energy under Contract No. DE-AC06-76L0-1830.

 0021-9606/94/101(9)/8138/14/$6.00

the dipole moment with the electric field due to other dipoles ($-\mu\cdot E$). This is actually the electrostatic energy to remove the dipole from a frozen array of the other dipoles. The difference between this quantity and the actual desorption activation energy is the relaxation energy of the vacancy created by a desorbed dipole.

Despite the many obvious limitations inherent in this simple electrostatic model,[19–21] its computational simplicity and easy empirical parameterization allows understanding of its effects on observations, and motivates us to treat it fully here, and present several useful analytic approximations. This is done specifically for a neutral dipolar adsorbate (some of the better prior treatments have been for charged nonpolar adsorbates, which yield different expressions, which have often been misapplied or mistranslated to the neutral dipolar case).

II. MODEL FOR DIPOLE INTERACTIONS NEAR METAL SURFACES

A. General approach

We assume that the direct electrostatic interactions act as a perturbation on the otherwise static chemical bond between the molecule and the surface. (Better treatments exist, such as on a jellium surface,[19,20] but the method is not analytic, nor easy.) Most of the simple treatments have assumed the molecule to be a point dipole. This leads to a questionable description of the dipole–dipole interaction at higher coverages and of the dipole–metal interaction at all coverages. In the Appendix we develop extended dipole versions of all the equations, and compare them with the point dipole versions. The conclusion reached is that typically the point dipole and extended dipole results are numerically very close. Thus in the main text we use the point dipole model, as it makes the relationships easier to grasp.

We use rationalized MKS units, except the polarizability α is in Å^3 (similar to cgs units). Dipole moments in all equations are in MKS (coul m), but in the text they are in D, with 1 D$=3.34\times10^{-30}$ coul m. Note that the seldom used α_{MKS} equals $(4\pi\epsilon_0)\cdot\alpha_{\mathrm{cgs}}$, where ϵ_0 is the vacuum permitivity.

B. Definition of model

We consider a hexagonal array of point dipoles, adsorbed on an ideal infinitely polarizable metal surface, with the dipole axis parallel to the surface normal and the negative end of the dipole closest to the metal. Thus the dipole vector points away from the surface. The center of each dipole is located a distance β from the image plane of the metal (the model is drawn in the Appendix for the extended dipole case, Fig. 7). Each molecule is assumed to have a fixed dipole moment μ_0 in the absence of an external electric field and a polarizability α which describes the change in dipole moment from μ_0 due to an external field

$$\Delta\mu=\mu_{\mathrm{ind}}=4\pi\epsilon_0\alpha E. \tag{1}$$

The field E above is the total external field including that due to the image of the dipole. Note that α for a real molecule is expressed as the rank 2 tensor α_{ij} (represented as a 3×3 matrix). Since the electric fields near a metal surface are predominantly along the surface normal (z direction) and we have constrained the dipole to be oriented perpendicular to the surface, α_{zz} will effectively determine $\Delta\mu$. The scalar α obtained from gas phase measurements is typically an angle averaged value. If the polarizability is completely isotropic, α_{zz} for an oriented dipole will correspond to the gas phase α. However, if for example the polarizability along the z axis dominants the tensor α_{ij}, α_{zz} is nearly three times the gas phase α. With this caution made, we will hereafter refer to α_{zz} simply as α. It is also likely that μ_0 and α will be perturbed from their gas phase values due to electronic structure changes caused by adsorption due to either charge transfer or covalent effects.

Each dipole induces a screening charge on the metal surface such that the parallel components of the electric field at the metal surface are zero. Using the method of images (Ref. 22, and the Appendix), the electric field above the metal surface is given by the sum of the fields from the dipole and a fictitious image dipole a distance β below the image plane, pointing in the same direction as the dipole. The electric field vector acting on a given dipole due to the *other* dipoles within the array thus points in the direction opposite that of that dipole.

C. Energy and polarization of a dipole in an electric field

The energy difference between a fixed (unpolarizable) point dipole in a uniform external electric field and the dipole in zero external field is given by the dot product of the field with the dipole moment

$$U_d=-\mu\cdot E. \tag{2}$$

If the dipole is polarizable along its axis, the electric field will induce a change in the dipole moment proportional to the electric field strength

$$\mu=\mu_0+4\pi\epsilon_0\alpha E. \tag{3}$$

The total energy within the electric field is not given by Eq. (2), however, since this does not account for the energy necessary to polarize the dipole from its field-free state. The change in internal potential energy is

$$U_p=\frac{(\mu-\mu_0)^2}{8\pi\epsilon_0\alpha}. \tag{4}$$

(See Refs. 15–17 and the Appendix for elaboration.) The polarization energy and the total energy of the dipole is then

$$U_p=\tfrac{1}{2}\cdot E(\mu-\mu_0), \tag{5}$$

$$U=-\mu\cdot E+\tfrac{1}{2}\cdot E(\mu-\mu_0)=-\tfrac{1}{2}E\cdot(\mu_0+\mu). \tag{6}$$

Shown in Fig. 1 is U for a dipole with $\mu_0=1.0$ D and $\alpha=7$ Å^3 with an external field E applied to oppose μ_0. For comparison, CH_3Br has a dipole moment μ_0 of 1.81 D and a polarizability α along the C–Br bond direction of 6.5–7.0 Å^3.[23,24] At low external field strengths, the energy is proportional to the applied field. As the field strength is further increased, the $\mu\cdot E$ term reaches a maximum, since the dipole moment decreases linearly with the field strength, even-

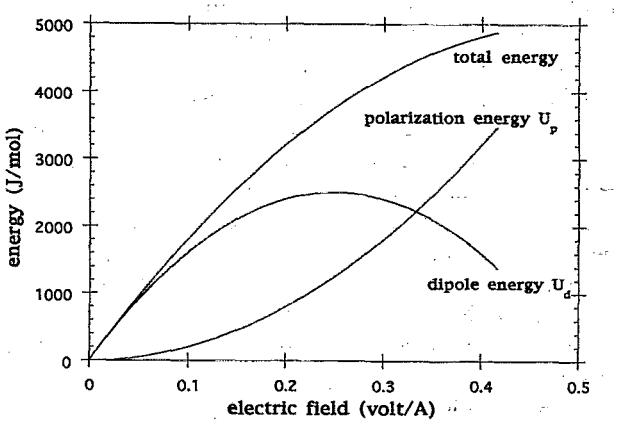

FIG. 1. Comparison of the relative contributions of simple dipole energy and polarization energy to the total potential energy for a dipole (μ_0=1.5 D, α=7 Å^3) oriented in opposition to a static uniform electric field.

tually crossing zero and reversing sign (however, the *self-generated* field from a polar layer can only push μ to zero, not beyond). The polarization energy is proportional to the square of $\Delta\mu$ at all field strengths, and thus will predominate when the dipole is substantially depolarized.

D. Potential energy for a dipole near a metal surface

A dipole oriented vertically near a metal surface is stabilized in energy due to the interaction with the screening (image) charge induced on the metal surface. The electric field E_{image} produced by the screening charge for a point dipole measured at the position of the point dipole is given by

$$E_{\text{image}}=\frac{\mu}{16\pi\epsilon_0\beta^3}. \tag{7}$$

β is the distance from the point dipole to the image plane. The screening charge also induces further polarization of the dipole. The dipole moment for the adsorbed dipole is given by inserting E_{image} into Eq. (3)

$$\mu=\frac{\mu_0}{1-[\alpha/(4\cdot\beta^3)]}. \tag{8}$$

Note that in this case μ is larger than μ_0. We then wish to obtain the total energy $U=U_{\text{se}}+U_p$ for the dipole near the metal. The first term is the energy of the dipole in its self-induced field

$$U_{\text{se}}=-\frac{1}{2}\left(\frac{\mu}{16\pi\epsilon_0\beta^3}\right)\cdot\mu. \tag{9}$$

The factor of 1/2 is required, as is typical for self-induced interactions like this charge-to-image-charge attraction (see the Appendix). The internal polarization energy of the molecule is in this case given by

$$U_p=\tfrac{1}{2}\cdot(\mu-\mu_0)\cdot E_{\text{image}}, \tag{10}$$

and therefore the total potential energy for an isolated dipole oriented vertically on a metal surface is

$$U=-\tfrac{1}{2}\cdot E_{\text{image}}\cdot\mu_0=-\frac{\mu_0^2}{8\pi\epsilon_0(4\beta^3-\alpha)}. \tag{11}$$

This dipole–metal interaction above will hold as well for the dynamical dipoles that form the basis for the dispersion forces. This has been shown to result in changes in dispersion forces near a metal, and also may account for how nonpolar species like Xe or N_2 acquire dipole upon adsorption.[25]

E. Potential energy due to other dipoles

We now wish to calculate the additional potential energy for an adsorbed dipole that results from electrostatic interactions with other dipoles in a two dimensional array of density n. Each dipole, in addition to the self-field E_{image}, is acted upon by an electric field E_d due to the sum over all other dipoles. This field has the general form

$$E_d=-\frac{\mu}{4\pi\epsilon_0}F(n), \tag{12}$$

where $F(n)$ depends on the geometry, but not on μ. The specifics of $F(n)$ will be considered shortly. First we consider the total electrostatic energy U per adsorbed dipole. This quantity, summed over all adsorbates, will give the total energy of the adsorbed layer due to electrostatic interactions. This will be comprised of three terms: the potential energy U_d of the dipole due to interactions with other dipoles; the self-image energy of the dipole U_{se}; and the polarization energy U_p. For the first term, a factor of 1/2 is included in the normal dipole energy expression to avoid double counting of the pairwise terms (consistent with our definition of energy/dipole). Thus

$$U_d=-\tfrac{1}{2}E_d\cdot\mu. \tag{13}$$

The total electrostatic potential energy per dipole is then

$$U_{\text{elec}}=-\tfrac{1}{2}E_d\cdot\mu-\tfrac{1}{2}E_{\text{image}}\cdot\mu+U_p \tag{14}$$

and the polarization energy U_p is

$$U_p=\frac{(\mu-\mu_0)^2}{8\pi\epsilon_0\alpha}=\tfrac{1}{2}E_t\cdot(\mu-\mu_0), \tag{15}$$

where $E_t=E_d+E_{\text{image}}$ is the total field acting to polarize the dipole. Thus the total electrostatic potential energy per dipole is

$$U_{\text{elec}}=-\tfrac{1}{2}(E_d+E_{\text{image}})\cdot\mu+\tfrac{1}{2}E_t\cdot(\mu-\mu_0)=-\tfrac{1}{2}E_t\cdot\mu_0. \tag{16}$$

This surprisingly simple expression fully accounts for all contributions to the electrostatic energy. The dipole moment μ is given by

$$\mu=\frac{\mu_0}{1+\alpha\left(F(n)-\dfrac{1}{4\beta^3}\right)} \tag{17}$$

and the field E_t is given by

$$E_t=-\frac{\mu}{4\pi\epsilon_0}\left(F(n)-\frac{1}{4\beta^3}\right)$$

$$= -\frac{\mu_0}{4\pi\epsilon_0}\left[\frac{1}{\left(F(n)-\frac{1}{4\beta^3}\right)^{-1}+\alpha}\right]. \tag{18}$$

We point out again that Eq. (16) accounts for all potential energy due to electrostatic (dipole) interactions, including self-image energy and polarization energy. The average adsorption energy for dipoles on a metal surface will consist of the sum of this term and a coverage-independent covalent term. To calculate $U_{\text{elec}}(n)$, we need to obtain the function $F(n)$ which describes the characteristics of the electric field due to other dipoles. Discussed in the following section are two approximation methods for calculating $F(n)$. The first of these is the commonly used discrete summation formalism[12–15] originally due to Topping. The second is an integral formalism developed here which more easily allows for incorporation of image dipole effects. The Appendix compares exact summations with these approximations.

III. ELECTRIC FIELD DUE TO AN INFINITE DIPOLE ARRAY

A. 2D point dipole lattice field including images

We now consider the specifics of the field due to an array of dipoles. The point dipole limit for the electric field due to an isolated point dipole vector μ, at a point a distance R along the plane bisecting the dipole, is

$$E=\frac{-\mu}{4\pi\epsilon_0 R^3}, \tag{19}$$

where E points in the direction opposite the dipole. If two aligned dipoles are positioned such that each is located the same distance β above the metal surface, there is an additional electrostatic interaction between each dipole and the screening charge (image) of the other. The net electric field acting on one of the dipoles is then given by the sum of the field from the other dipole, the field due to the image of the other dipole, and that due to the self image of the dipole itself. Each of these components to the electric field will also contribute to the polarization of each dipole.

B. Topping method for dipole array

To calculate the electric field acting on a dipole within an infinite array of dipoles, it is necessary to sum the individual electric fields due to each of the other dipoles. For a layer consisting of mobile aligned dipoles, the lowest energy arrangement is a hexagonal array. For such a layer with a two-dimensional density n, *if interactions due to image charges are neglected*, this infinite summation over all other dipoles is easy to perform. The electric field acting on a dipole is given by

$$E=\frac{-\mu}{4\pi\epsilon_0 R_s^3}\cdot\sum_{-\infty}^{+\infty}\sum_{-\infty}^{+\infty}(j^2+k^2-jk)^{-3/2} \tag{20}$$

where $R_s(n)$ is the nearest-neighbor distance in the dipole array and j and k are integers which are not equal to zero simultaneously. Evaluation of the double summation yields a value very close to 11.03. For a hexagonal array, $R_s(n)$ can be expressed as a function on the dipole density n

$$R_s(n)=\frac{(4/3)^{0.25}}{\sqrt{n}}. \tag{21}$$

Insertion of this into Eq. (19) yields a convenient expression for the coverage-dependent field (with images neglected)

$$E=-\frac{11.03\mu}{4\pi\epsilon_0 R_s^3} \tag{22}$$

and by utilizing Eq. (3) and substituting $R_s(n)$ from Eq. (21) the self-consistent dipole moment as a function of dipole density is obtained

$$\mu(n)=\frac{\mu_0}{1+8.89\alpha n^{3/2}}. \tag{23}$$

Note that $F(n)=8.89n^{3/2}$ for this case. This method yields a simple expression because the summation term can be separated from the simple $1/r^3$ point dipole field term. This is not the case if the electric field due to *image* charges of the other dipoles is included. We introduce below an integral formalism which allows us to obtain a simple analytical approximation to the electric field including the image charge effects.

C. Integral method for dipole array

We postulate that there is a distance R_s', also proportional to the inverse root of the surface density,

$$R_s'=C\cdot R_s, \tag{24}$$

which satisfies the condition that the integral of the electric field acting on a point in the dipole array, due to a uniform dipole density on the surface (equal to μn) over the region from $R=R_s'$ to R=infinity (over 2π radians), is approximately equal to the summation of the individual electric fields, acting on the same point on the surface, due to discrete dipoles separated by nearest neighbor spacings of R_s as given by Eq. (22) for the hexagonal lattice. Note that R_s' will likely be different than R_s. For the case of point dipoles (no images), the integral formalism for the same lattice is

$$E(n)=\int_{R_s'}^{\infty}\int_0^{2\pi}\frac{-\mu\cdot n}{4\pi\epsilon_0 R^3}\,R\,d\theta\,dR. \tag{25}$$

Performing the above integration yields the following:

$$E(n)=\frac{-\mu n}{2\epsilon_0 R_s'}. \tag{26}$$

Upon substituting in R_s' from Eq. (24) and using Eq. (21) solved for n, we obtain

$$E(n)=\frac{-\mu}{\sqrt{3}\epsilon_0 C R_s^3}. \tag{27}$$

If we compare this result with that in Eq. (22) (the Topping result), it is evident that the two expressions are equal if $C=2\pi/9.95=0.658$; thus $R_s'=0.658R_s$.

D. Electric field including image charges

The utility of the integral approach is that it can also be employed when the dependence of the field on dipole separation distance R is more complex; such is the case if interactions with the dipole images are included. The z component of the electric field acting on a point dipole due to second point dipole (with both located a distance β above a metal surface) and the image of the second dipole is given by[15]

$$E=-\frac{\mu}{4\pi\epsilon_0}\cdot f(R), \tag{28}$$

where

$$f(R)=\frac{1}{R^3}-\frac{3(2\beta)^2}{[R^2+(2\beta)^2]^{5/2}}+\frac{1}{[R^2+(2\beta)^2]^{3/2}}.$$

The first term in $f(R)$ is the usual dipole–dipole field term whereas the second and third terms account for the z component of the electric field due to the neighbor's image dipole. Note that the image of a neighboring dipole also will produce an electric field component perpendicular to the dipole orientation (and a torque on the dipole), but this will effectively sum to zero for a dipole symmetrically surrounded by other dipoles on a surface. However, this might be a more important consideration when calculating electric fields in the vicinity of a cluster of dipoles on a surface, for example, or in other cases where symmetry is absent.

The general procedure for determining the total dipole-induced electric field involves performing the following integration:

$$E(n)=\frac{-\mu n}{4\pi\epsilon_0}\int_{R_s'}^{\infty}\int_0^{2\pi} Rf(R)d\theta\, dR. \tag{29}$$

This will yield three terms [one for each of the three terms in $f(R)$]. We already have accounted for the first of these [the result of performing the integration in Eq. (25)]; this is the field due to the other (real) dipoles

$$E_1(n)=\frac{-\mu n}{2\epsilon_0 R_s'}. \tag{30}$$

The remaining terms corresponding to the image dipoles can be integrated similarly. For the second term, we have

$$E_2(n)=\frac{\mu n}{4\pi\epsilon_0}\int_{R_s'}^{\infty}\int_0^{2\pi}\frac{3(2\beta)^2}{[R^2+(2\beta)^2]^{5/2}}R\, d\theta\, dR$$

$$=\frac{\mu n}{\epsilon_0}\frac{2\beta^2}{[(R_s')^2+(2\beta)^2]^{3/2}}. \tag{31}$$

The partial field corresponding to the third term is then obtained

$$E_3(n)=\frac{-\mu n}{4\pi\epsilon_0}\int_{R_s'}^{\infty}\int_0^{2\pi}\frac{1}{[R^2+(2\beta)^2]^{3/2}}R\, d\theta\, dR$$

$$=\frac{-\mu n}{2\epsilon_0}\frac{1}{[(R_s')^2+(2\beta)^2]^{1/2}}. \tag{32}$$

Therefore, the total field E_d due to other dipoles is the sum of E_1, E_2, and E_3

$$E_d(n)=\frac{-\mu n}{2\epsilon_0}\left[\frac{1}{R_s'}-\frac{4\beta^2}{[(R_s')^2+(2\beta)^2]^{3/2}}+\frac{1}{[(R_s')^2+(2\beta)^2]^{1/2}}\right]. \tag{33}$$

We then substitute in R_s' and n as before and rearrange into the form given by Eq. (12)

$$E_d(n)=\frac{-\mu}{4\pi\epsilon_0}F(n),$$

where

$$F(n)=\frac{4\pi}{\sqrt{3}\cdot CR_s^3}\left(1+\frac{1}{\left[1+\left(\frac{2\beta}{CR_s}\right)^2\right]^{3/2}}\right). \tag{34}$$

We can show that Eq. (34) has the same limits as the Topping expression for β approaching either infinity or zero

$$\underset{\beta\to\infty}{\text{LIMIT}}[E_d(n)]=\frac{-\mu^2}{4\pi\epsilon_0}\cdot\frac{11.03}{R_s^3} \tag{35}$$

and

$$\underset{\beta\to 0}{\text{LIMIT}}[E_d(n)]=\frac{-\mu^2}{4\pi\epsilon_0}\cdot\frac{22.06}{R_s^3}. \tag{36}$$

The limit in Eq. (36) is expected to be twice that for the infinite limit since the field results from two dipoles (real and image) at the same location in space. Therefore, setting $C=0.658$ is accurate at both the limits, and thus we expect it to be a good estimate at intermediate values of β (see the Appendix for comparisons).

IV. TOTAL BINDING ENERGY AND INTERACTION ENERGY

Insertion of the expression for $F(n)$ as given in Eq. (34) into Eqs. (16)–(18) from Sec. II E yields the coverage dependent electrostatic potential energy

$$U_{\text{elec}}=\frac{\mu_0^2}{8\pi\epsilon_0}\left(\frac{1}{\left[F(n)-\frac{1}{4\beta^3}\right]^{-1}+\alpha}\right),$$

with

$$F(n)=\frac{4\pi}{\sqrt{3}\cdot CR_s^3}\left(1+\frac{1}{\left[1+\left(\frac{2\beta}{CR_s}\right)^2\right]^{3/2}}\right)$$

and

$$R_s(n)=\frac{(4/3)^{0.25}}{\sqrt{n}},\quad C=0.658. \tag{37}$$

The total adsorption energy U_{tot} includes the covalent (or physisorption) energy U_{cov} which for simplicity we assume

is a constant. This assumption is most likely a gross simplification for two reasons. First, the local electronic structure of the metal surface near a chemisorbed dipole will quite likely be perturbed by the presence of other nearby dipoles. Second, it is probable that the extent of covalent bonding will change upon polarization of the dipole. Note that this is distinct from the change in the electrostatic self-image energy of the dipole. The coverage dependent $U_{tot}(n)$ is

$$U_{tot}(n)=U_{elec}(n)+U_{cov}. \tag{38}$$

$U_{tot}(n)$ is approximately equal to the thermodynamic adsorption energy per dipole and will determine the equilibrium properties for coadsorbed systems. A quantity often of interest is the change in the adsorption energy from the zero-coverage limit due to the proximity of the other dipoles. This is generally termed the interaction energy U_i and is obtained by subtracting the adsorption energy for a dipole isolated on the surface ($n=0$) from that at a given density n.

$$U_i(n)=U_{tot}(n)-U_{tot}(n=0)=-\tfrac{1}{2}E_t\cdot\mu_0+\tfrac{1}{2}E_0\cdot\mu_0. \tag{39}$$

The first term on the right of Eq. (39) is $U_{elec}(n)$. Since there are no dipole–dipole terms in the zero coverage limit, the second term is simply the self-image energy for a isolated dipole. E_0 is the self-induced field ($E_0=E_{image}$ for an isolated adsorbed dipole). Also, there have been examples in the literature of the formation of ordered structures of two coadsorbed species with dipoles pointing in opposite directions. To compare the relative stability of various overlayer structures, it is necessary to compare $U_{tot}(n)$ for each of the structures.

V. DISCUSSION

A. Dipole polarization energy and self-image energy

We first show that the magnitudes of the polarization energy and the self-image energy change relative to the potential energy due to other dipoles can be significant for physically reasonable values of α, β, and the dipole density n. Obtaining appropriate values for β (the distance from the dipole center to the image plane) is problematic, but values in the range of 2–3 Å are not unreasonable. The three contributions to the electrostatic energy for $\mu_0=1.5$ D, $\alpha=7$ Å^3, and $\beta=2.5$ Å are compared in Fig. 2. The magnitude of the dipole–dipole energy (U_d) reaches a maximum near coverages of 5×10^{14}/cm^2, and the polarization energy U_p can exceed 50% of U_d. The minimum in U_p occurs because the dipole near zero coverage is polarized to a value greater than μ_0 by the self-image field. The self-image energy U_{se} is attractive at all coverages (since the dipole is never fully depolarized) but decreases in magnitude by nearly 50% at the highest coverages. The choice for β has a large effect on both U_d and U_{se}, as shown in Fig. 3. The increase of the magnitude of the self-image energy U_{se} as β is decreased dominates the overall energy change, but this is somewhat moderated by the increase in U_d. The increase in the dipole–dipole interactions occurs because the self-image interaction causes the dipole to polarize to increasingly larger values. It

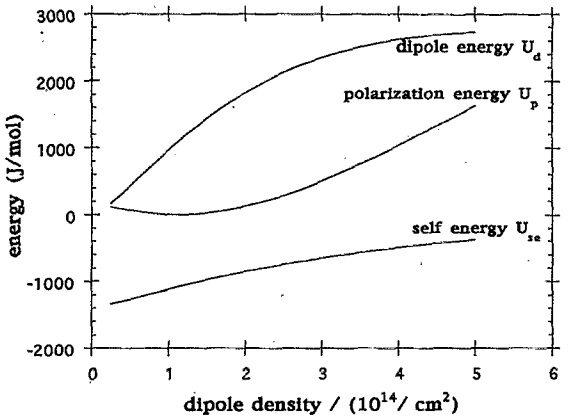

FIG. 2. Comparison of the dipole energy U_d (a), the polarization energy U_p (b), and the self-image energy U_{se}, (c) for a dipole array on a metal surface as a function of dipole density with $\mu_0=1.0$ D, $\alpha=7$ Å^3, and $\beta=2.5$ Å.

is therefore clear that the self-image induced effects can play a large role in determining the net interaction between dipoles.

Some authors have computed electric fields and dipole moments using an "effective" polarizability for the dipole surface complex.[11,15] We will not digress to discuss the validity or usefulness of this, except to note that the coverage dependence of the self-image energy is neglected using such a procedure.

B. Thermal desorption kinetics

Desorption kinetics are often analyzed in terms of an Arhennius rate expression, with the "activation energy" U_a often equated with the adsorption energy

$$\frac{dn}{dt}=-n\nu\exp\left(\frac{-U_a(n)}{RT}\right), \tag{40}$$

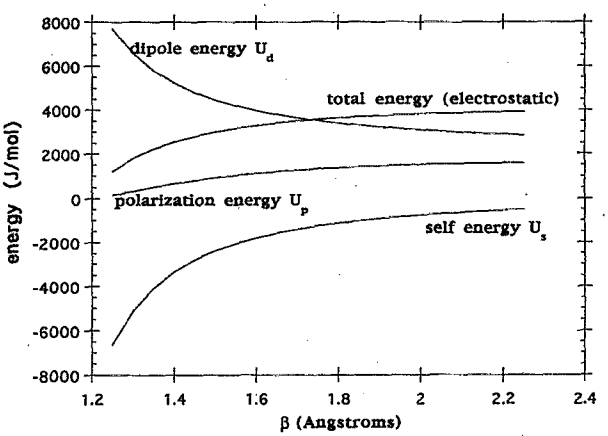

FIG. 3. Comparison of the dependence on β of the various contributions to the total electrostatic energy. (a) total energy U, (b) dipole energy U_d, (c) polarization energy U_p, (d) self-image energy U_{se}. $\mu_0=1.5$ D, $\alpha=7$ Å^3, and $n=5\times10^{14}$/cm^2.

where n is the coverage (per unit area), the desorption is here assumed to be first order with respect to coverage, and the activation energy is coverage dependent. This is a simplistic model, neglecting many important phenomena.[26] It is however often a useful empirical fitting equation, with physically reasonable parameters. Equation (38) gives the binding energy per adsorbate $U_{\rm tot}(n)$. Qualitatively one should expect the *differential* adsorption energy $|d[nU_{\rm tot}(n)]/dn|$ to relate to U_a.[26]

This expectation is made more rigorous by appealing to thermodynamics. For an ideal gas in equilibrium with a surface the temperature dependence of the pressure at constant coverage is given by

$$\frac{d[\ln(p)]}{d(1/T)}=\Delta H_{\rm iso}(n), \tag{41}$$

where $\Delta H_{\rm iso}(n)$ is the coverage dependent *differential* isosteric enthalpy of adsorption (the heat released per molar increment of surface coverage at constant T, P, and surface area).[27] If one sets up an equilibrium using Eq. (40) and an ideal gas, with a constant sticking probability, the pressure–temperature coverage relationship derived is similar to that in Eq. (41) with $U_a(n)$ set equal to $\Delta H_{\rm iso}(n)$ (ignoring slowly varying T dependent terms). Now $\Delta H_{\rm iso}(n)$ differs from the thermodynamic adsorption energy by about RT, which is typically only 3% to 5% of $\Delta H_{\rm iso}(n)$ at the desorption temperatures in TPD. So we find that the thermodynamic *differential* adsorption energy should be approximately equal to $U_a(n)$ in TPD analysis

$$U_a\approx\frac{-d[nU_{\rm tot}(n)]}{dn}=\frac{-d[nU_{\rm elec}(n)]}{dn}-U_{\rm cov}. \tag{42}$$

Unfortunately, the derivative of $nU_{\rm elec}$ is algebraically long and tedious. Our recommendation is to numerically differentiate $nU_{\rm elec}$ to evaluate U_a.

As discussed in Sec. I, there have been many efforts at modeling the apparent coverage dependence of U_a.[1,3,4] In all cases, the polarization energy and self-image energy change were not included in the model for the dipole–dipole destabilization. Thus far we have shown that these can be significant components of the total interaction potential and should be an important consideration when analyzing thermal desorption data. However, there is an additional aspect to the desorption problem which has previously been treated incorrectly. It is generally assumed that the coverage dependent part of U_a is simply equal to $E_d\cdot\mu$ (that is, the energy of the dipole in an electric field). We will show below that this approach actually yields a quantity which is different from $U_a(n)$ as given by Eq. (42).

C. Adiabatic versus sudden desorption

Another way to evaluate the desorption barrier is to calculate stepwise the energy changes upon removal of one adsorbate from the surface and leaving the rest behind. If done correctly, this will equal the derivative of $nU_{\rm elec}$. However, several treatments have assumed that the coverage dependent part of this energy is simply μ dotted into the electric field due to the other dipoles, or $E_d\cdot\mu$. This is not correct, first

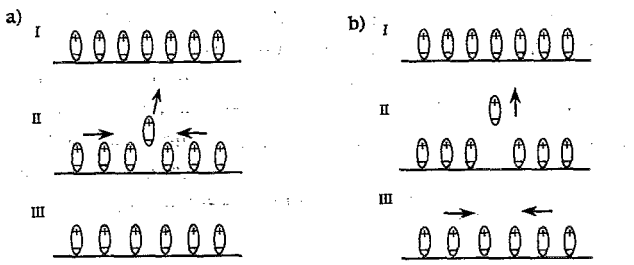

FIG. 4. Two possible desorption mechanisms: (a) adiabatic, where lateral diffusion of dipoles to fill vacancy occurs concurrently with desorption (step II), (b) sudden, where lateral diffusion to fill vacancy occurs subsequent to the desorption event (step III).

because the self-energy is coverage dependent. Second, and more subtly, it leaves the surface in a final state of an adsorbate *vacancy*, with the position and dipole moment μ of the neighboring molecular dipoles fixed at the values for the dipole layer with no vacancy. The activation energy from this approach we will call $U_{\rm sud}$, for "sudden," as one can suggest that the desorption is so sudden that the vacancy does not have time to heal on the time scale of the desorption (nor alter their polarization). Our calculation via the derivative of $nU_{\rm tot}$ clearly leaves the surface with the vacancy "healed." We can refer to this latter assignment of the activation energy U_a as $U_{\rm adiab}$, where the desorption is "adiabatic." It takes energy to create the sudden vacancy, so $U_{\rm sud}>U_{\rm adiab}$. These two physical scenarios are shown in Fig. 4. This sudden scenario is not likely to be correct in that the electronic polarization should always be adiabatic. However, it is arguable that in an actual desorption that the final state *is* a physical vacancy, i.e., the healing of the vacancy will take place on a time scale such that the associated energy can not contribute to the molecule's desorption.

The difference between the sudden and adiabatic energies is significant. We will examine a simple limit where this difference is qualitatively clear, and algebraically simple. In the limit of low coverage, $F(n)$ in Eq. (35) approaches $2\pi Cn^{3/2}$. Then the field at an adsorbate due to its neighboring dipoles E_d is proportional to $n^{3/2}$. If we further assume that α is zero, the self-image field $E_{\rm image}$ is independent of n and the problem of "sudden" electronic rearrangement is avoided. Starting with Eq. (37) we can get a simple expressions for $U_{\rm adiab}$. We first rewrite $U_{\rm tot}$ by separating the dipole term from the self-field term

$$U_{\rm tot}=[-\tfrac{1}{2}E_d\cdot\mu_0-\tfrac{1}{2}E_{\rm image}\cdot\mu_0]+U_{\rm cov}. \tag{43}$$

(For $\alpha=0$ and small n):

$$U_{\rm adiab}\approx-\frac{d(nU_{\rm tot})}{dn}\approx[\tfrac{5}{4}E_d\cdot\mu_0+\tfrac{1}{2}E_{\rm image}\cdot\mu_0]-U_{\rm cov}. \tag{44}$$

In the sudden desorption limit, the neighboring molecules have their polarization frozen at the value held before the central molecule desorbs; thus $U_{\rm sud}$ is easy to calculate. The change in energy includes the loss of the covalent interaction, the self-image energy, and also the repulsive energy

of a dipole in a static field due to the other dipoles. This latter term is given by precisely $E\cdot\mu_0$. This lacks the factor of one half seen in Eq. (13), since when we remove this molecule we completely lose the interaction with all other dipoles. Note that we have also included the polarization energy (by using $E_d\cdot\mu_0$ instead of $E_d\cdot\mu$) and the self-image energy in the expression for $U_{\rm sud}$ in

$$U_{\rm sud}=[\tfrac{1}{2}E_d\cdot\mu_0+\tfrac{1}{2}E_t\cdot\mu_0]-U_{\rm cov}. \tag{45}$$

Comparing Eqs. (44) and (45), and remembering that $E_d\cdot\mu$ is negative while all these activation energies are positive, we see that $U_{\rm sud}$ is greater than $U_{\rm adiab}$ by $(1/4)|E_d\cdot\mu|$ (at low densities and with α set to zero). This is the energy to create a vacancy. Thus the energy to create the vacancy is half the average lateral dipole–dipole repulsion.

It might be argued that in desorption a vacancy should indeed be left behind, so that maybe we should really use $U_{\rm sud}$. However, we can use microscopic reversibility to show that this not the case. If desorption typically occurs with a direct trajectory away from the surface to leave a vacancy, then the reverse scenario must be true for adsorption; i.e., for a molecule to adsorb it must hit a preexisting vacancy. If vacancies have a significant energy associated with their creation, they should be rare, and thus the sticking probability should be much less than one. However, most molecules with large dipole moments have sticking probabilities which are near unity at all coverages. The typical adsorption event will more likely involve a collision with the existing overlayer which will have considerable variability in configuration. The collision will be accompanied by internal and molecule-to-surface energy exchange, diffusion, binding in weaker adsorption wells, etc., before the molecule finally settles into the adsorbate layer. The adsorption trajectory is thus tortuous, as will be the reverse desorption process, with many returns and resamplings of the Boltzmann distribution. This makes the overall kinetics insensitive to the adiabatic/sudden issue above. The "transition state" exists well beyond this step, and the intermediate states will be populated in an equilibrium Boltzmann distribution. Thus the adiabatic (thermodynamic) activation energy, $U_a=U_{\rm adiab}$, is the proper one to use.

We have used Eqs. (44) and (45) to calculate the coverage dependent decrease in the desorption barrier (from the zero coverage limit of U_a) predicted for the cases of adiabatic and sudden desorption. To further demonstrate the importance of including the polarization energy U_p and the self-image energy U_s, we have also performed the calculation for the same two cases with the U_p and the U_s neglected. These are compared in Fig. 5. For the complete classical model (traces a and b), the difference between the adiabatic and sudden desorption models is approximately 10%. Where the incomplete models are compared (c and d), unusual behavior is observed; the relative magnitudes for the adiabatic and sudden cases are reversed. Note that the incomplete adiabatic model (curve c) predicts a minimum in the desorption barrier at half of saturation coverage. This unrealistic prediction occurs specifically due to the neglect of polarization energy.

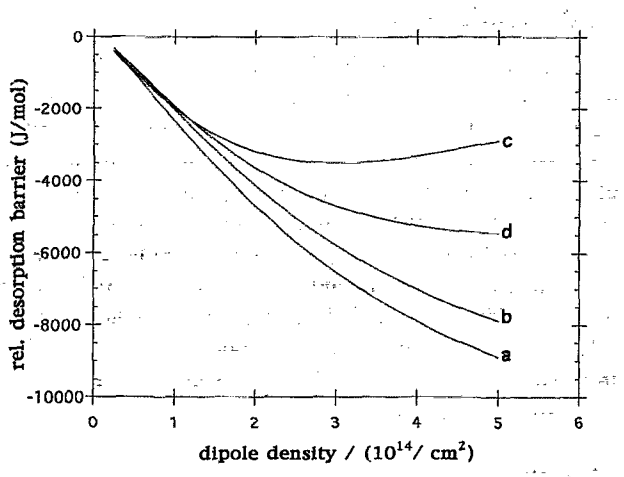

FIG. 5. Change in desorption barrier U_a with coverage for (a) complete adiabatic desorption model, (b) complete sudden desorption model, (c) adiabatic desorption model with polarization and self-image energy change neglected, and (d) sudden desorption model with polarization and self-image energy change neglected. μ_0=1.5 D, α=7 Å^3, and β=2.5 Å.

Shown in Fig. 6 are calculated temperature programmed desorption traces corresponding to the four desorption barrier profiles in Fig. 5. We have assumed a zero coverage binding energy of 4.8 kJ/mol, a constant pre-factor ν of 10^{13} s^{-1}, and a linear temperature ramp of 5 K/s. The fourth order Runge–Kutte method was used for the numerical integration. As expected, there is a significant difference between the line shapes for the various models, although the difference between the complete adiabatic and sudden models (curves a and b) is probably much less than the inaccuracies of the classical model in general. When applying these models in a least-squares fitting scheme of TPD data, it is likely that each of these models can be parameterized to fit the data reasonably well, but the resultant parameters will be quite different.

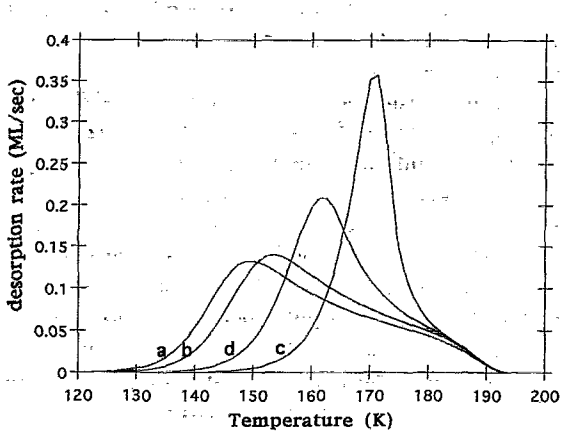

FIG. 6. Calculated temperature programmed desorption line shapes using the coverage dependent desorption barrier models in Fig. 6.

VI. CONCLUSIONS

The classical point dipole on a perfect metal electrostatic model can be expressed in a simple analytical form, and without a variety of approximations/errors that have plagued these simple models. We have demonstrated the importance of including the energy required to polarize a dipole as well as the change in the self-image electrostatic energy due to polarization in the total dipole interaction energy. The application of the model to phenomena such as thermal desorption is straightforward, but it is necessary to clearly define the relevant energy changes. In the Appendix, we show that using extended dipoles also leads to simple expressions, and compare various approximations.

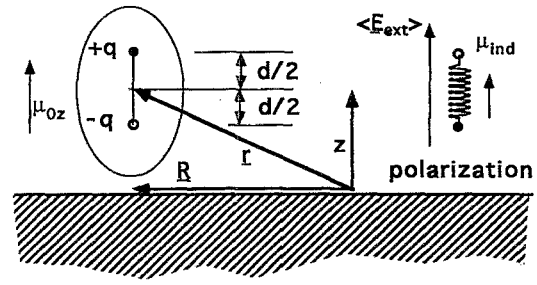

FIG. 7. Coordinates for extended dipole above a surface.

APPENDIX

This Appendix has three functions: (1) to set up and examine the physical model used for the polarizable dipole; (2) to develop extended dipole versions of the simpler point dipole equations of the main text; (3) to numerically compare the point and extended results, including various analytical approximations for these equations.

Physical model

Springs and charges

Knowing a molecule's dipole moment and polarizability does not provide us with sufficient information to predict lateral interactions, even when one assumes that these interactions are purely electrostatic. Beyond the obvious need for more spatial information on the charge and polarizability, lateral interactions are calculable only if we create a *physical* model for the molecules, which then we permit to interact via classical or quantum mechanics. The dipole moment and polarizability are then used to set values for physical charges, springs, etc. The point dipole/polarizability representation widely used (as in the main text) is convenient due to the simplicity of the resulting equations. However the charge distribution in molecules responsible for these properties are of a similar size as the spacing between the adsorbed molecule and the surface at any coverage, or between adsorbates at high coverages. So any point model may be of questionable use. We develop a simple extended model, to numerically assess the differences between it and point dipole/polarizability models.

A second advantage of the extended model is that it is completely calculable. The point dipole/polarizability model possesses many infinities and infinitesimals (not uniquely defined either) such that it is difficult to answer many physical questions that would be trivial for an extended system, some of which serve as excellent "checks" of the correctness of the treatments. This is part of the reason that so many mistakes have been made in published dipole interactions treatments. The extended model results conveniently yield the point limit by then setting d to zero with $|\mu_0|$ held constant.

The extended physical representation we use is two point charges of opposite sign placed one on each end of a spring. It has both an unperturbed (zero external field) dipole moment and a polarizability. An external field will change the equilibrium spring length, thus the dipole moment. After understanding its properties, we then replace it with a model of two charges at the ends of a fixed length stick, the charges changing value upon application of external fields to reproduce the polarizability. This saves much algebra, and is basically a first to second order expansion of the charges-on-spring model.

Figure 7 shows the coordinates used. An adsorbate molecule is assumed to have an unperturbed dipole moment μ_0, oriented perpendicular to the surface. This dipole is modeled by two point charges $+/-q$ located d apart ($qd=|\mu_0|$), centered about the end of the vector $\mathbf{r}$, which gives the molecule's nominal position. The point dipole case is obtained in the limit of $d\rightarrow 0$ with $|\mu_0|$ fixed.

This molecule is able to polarize in response to an electric field applied externally. We anticipate that a phenomenological scalar polarizability α exists, such that an external electric field will induce in this molecule a dipole of strength $\mu_{\text{ind}}=(4\pi\epsilon_0\alpha)\langle\mathbf{E}_{\text{ext}}\rangle$. The corner-bracketed field means some sort of "averaged" field acting on the dipole. (Our definition of averaged will be a matter of future convenience.) This is shown at the right side of Fig. 7.

The charges are attached to a spring, with spring constant $\mathbf{a}'$ and length at zero force of d_{zf}. The force on the top charge will consist of three terms, the $+q$ to $-q$ attraction, the spring force, and the force from the externally applied field $q\mathbf{E}_{\text{ext}}$. For the case with zero external field, the molecule reaches an equilibrium at $d=d_0$ with the compressed spring force balancing the $+q$ to $-q$ attraction. Around the equilibrium position the net forces are to lowest order usually harmonic. To the extent that the system can be modeled as having linear polarizability, we can without loss of generality expand energies to second order in displacements. The "effective" or "net" spring constant $\mathbf{a}$ around the equilibrium d_0 (at zero external field) will contain both the spring constant $\mathbf{a}'$, and the second derivative of the $+q$ to $-q$ Coulombic attraction potential. Thus in Eq. (A1), the "bare" spring's potential energy is expressed (to second order) in the square brackets in terms of $\mathbf{a}$ and Coulombic derivatives. As a further convenience, we make sure that a change in d due to polarization does not move the center of the dipole; i.e., we force the two charges to move antisymmetrically about $\mathbf{r}$ (physically achievable in principle via mechanical pulleys).

Positioning the molecule far from the surface, we apply a fixed external field. The energy this gives for both charges,

compared to the energy possessed when $\mathbf{E}_{ext}$ and Φ_{ext} are zero is

$$\Delta U = \left\{ \frac{-q^2}{4\pi\epsilon_0 d} + \left[q^2(1-(d-d_0)/d_0+(d-d_0)^2/d_0^2)/4\pi\epsilon_0 d_0 + \frac{a(d-d_0)^2}{2} \right] + q\Phi_{ext}\left(\mathbf{r}+\zeta\frac{d}{2}\right) - q\Phi_{ext}\left(\mathbf{r}-\zeta\frac{d}{2}\right) - \left\{ \frac{-q^2}{4\pi\epsilon_0 d_0} + \left[\frac{q^2}{4\pi\epsilon_0 d_0}\right] \right\} \right\}, \tag{A1}$$

where ζ is a unit vector in the z direction. The square bracketed terms in Eq. (A1) are the spring's potential energy. The curly-bracketed terms are the total energy before and after imposing the external field. We look for that d which minimizes the energy. Here we introduce a convenient definition for $\langle \mathbf{E}_{ext} \rangle$, and an approximation (exact if the field is uniform)

$$\langle \mathbf{E}_{ext} \rangle \equiv \frac{\left(\Phi_{ext}\left(\mathbf{r}+\zeta\frac{d_0}{2}\right) - \Phi_{ext}\left(\mathbf{r}-\zeta\frac{d_0}{2}\right) \right)}{d_0}, \tag{A2a}$$

$$\left(\Phi_{ext}\left(\mathbf{r}+\zeta\frac{d}{2}\right) - \Phi_{ext}\left(\mathbf{r}-\zeta\frac{d}{2}\right) \right) \approx \frac{d}{d_0}\left(\Phi_{ext}\left(\mathbf{r}+\zeta\frac{d_0}{2}\right) - \Phi_{ext}\left(\mathbf{r}-\zeta\frac{d_0}{2}\right) \right) = -d\langle \mathbf{E}_{ext} \rangle, \tag{A2b}$$

$$= \Delta U(d) \approx \frac{a(d-d_0)^2}{2} - qd\zeta\cdot\langle \mathbf{E}_{ext} \rangle \quad [\text{to second order in } (d-d_0)], \tag{A2c}$$

$$\frac{\partial[\Delta U(d)]}{\partial d} = 0 \Rightarrow a(d_1-d_0) \approx q\langle \mathbf{E}_{ext} \rangle_z \Rightarrow \Delta\boldsymbol{\mu} = \boldsymbol{\mu}_{ind} \approx \frac{q^2}{a}\zeta\langle \mathbf{E}_{ext} \rangle_z, \tag{A2d}$$

$$\therefore (4\pi\epsilon_0)\alpha = \frac{q^2}{a}, \tag{A2e}$$

$$\therefore \Delta U(d_1) \approx \frac{1}{2}\boldsymbol{\mu}_{ind}\cdot\langle \mathbf{E}_{ext} \rangle - (\boldsymbol{\mu}_{ind}+\boldsymbol{\mu}_0)\cdot\langle \mathbf{E}_{ext} \rangle = -\frac{1}{2}\boldsymbol{\mu}_{ind}\cdot\langle \mathbf{E}_{ext} \rangle - \boldsymbol{\mu}_0\cdot\langle \mathbf{E}_{ext} \rangle. \tag{A2f}$$

Equation (A2c) expands the coulombic energy to second order in the displacement, which, as intended, cancels terms from the spring potential. In the above, the phenomenological polarizability is related to the spring constant. This can be used to write the change in the sum of the spring's potential energy plus internal $+q$ to $-q$ potential as $a(d-d_0)^2/2=(\mu-\mu_0)^2/2/(4\pi\epsilon_0\alpha)$. Equation (A2f) is consistent with the well established factor of 0.5 in front of the *induced* dipole energy term [see Refs. 16–18].

When $(d)E_{ext}(r)$ varies with r, expanding $\langle E_{ext} \rangle$ as in Eq. (A2b) gives much better results than using, for example, $(d)E_{ext}(r)$. This is because using $(d/d_0)\langle E_{ext} \rangle$ involves linear extrapolation of $[\Phi_{ext}(r+\zeta d_0/2)-\Phi_{ext}(r-\zeta d_0/2)]$ only over the distance Δd, instead of linearly extrapolating $E_{ext}(r)$ over the distance $+/-d/2$.

One can easily show that this charge-on-spring physical model is consistently well behaved, as are the phenomenological polarizability α and $\boldsymbol{\mu}_0$, to the extent that one can expand the energy up to quadratic terms in the change in dipole moment. However, the model becomes algebraically messy when one optimizes energies due to extended dipole potentials which contain terms like $1/(R^2+d^2)^{1/2}$. We now change the polarization's physical model so that an applied field does not change the distance d but instead changes the charges $+/-q$. This simplifies the algebra greatly, and generally gives the same results (at least to second order in displacements). This is more an algebraic trick rather than a physical model, since physically realistic capacitance to external objects requires *laterally* extended charges, of a size comparable to the molecular diameter, making the lateral interactions even more difficult to calculate. This gives the same expression for the polarization energy, $(\boldsymbol{\mu}-\boldsymbol{\mu}_0)^2/2/(4\pi\epsilon_0\alpha)$, in terms of the phenomenological α.

From Eq. (A2), it is fairly clear that any physical system or model (at least a nondegenerate one), which is initially in equilibrium, will exhibit: linear polarizability for small perturbations, interactions of the form of Eq. (A2), and a change in internal energy given by $(\boldsymbol{\mu}-\boldsymbol{\mu}_0)^2/2/(4\pi\epsilon_0\alpha)$. The latter is also clear via an external work analysis [see, for example, Ref. 17]. Our system is clearly in internal equilibrium. The point dipole/polarizability representation is *not* clearly in equilibrium given the infinities and infinitesimals (if one examines the system only after it is taken to the point limit). Arguments can ensue about whether certain internal coulombic interactions exist, or have already been implicitly accounted for in the model. Examination of Eq. (A2) for the *extended* system shows that as we let d_0 go to zero (holding $\boldsymbol{\mu}_0$ and α constant), the internal coulombic energy goes to infinity. And more importantly, so does the *change* in internal coulombic energy due to a finite external field. But the change in internal spring energy $a'(d-d_{zf})^2/2$ goes to infinity too. But this is not a problem, as the *sum* of these two terms is finite, giving $a(d-d_0)^2/2=(\boldsymbol{\mu}-\boldsymbol{\mu}_0)^2/2/(4\pi\epsilon_0\alpha)$. Thus examination of the extended system helps to reassure one that, even in the point limit, internal equilibrium is obtainable, and while the absolute change in internal coulombic energy is very model dependent, the more important change in *total* internal energy is model independent.

Method of images

When one has a group of point charges near a perfect metal (infinite polarizability) the electric field must be zero magnitude for $z<0$ and have no components along the surface at $z=0$. This field is achieved by a specific distributionof induced charge on the metal surface. It is well known that this field (in the region above the metal surface) is identical to that given by the original charges plus a group of fictitious charges: one per each real charge but of opposite sign, and each located as far below the surface plane as the

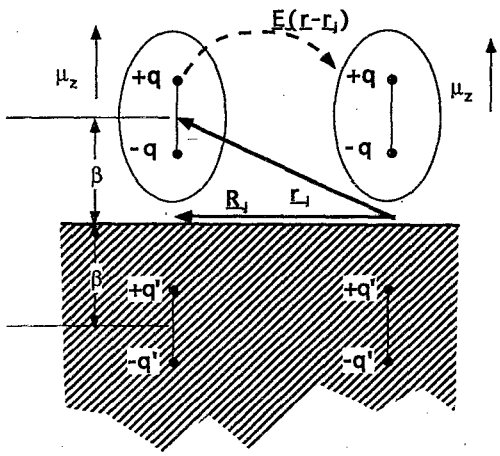

FIG. 8. Schematic of the electrostatic interaction between two adsorbed dipoles.

real charge is above it. This is the very venerable "method of images".[22] The resultant potential energy, compared to the charges dispersed infinitely from each other and the surface, is not so well known. Recalling from basic electrostatics that the energy change in an electric field is calculated by the change in the volume integral of E^2, and recalling that the field $E(r)$ is precisely zero in half of space, one can conclude immediately that the actual potential energy is one half that if all the charges were real. Thus the potential is 0.5*(real to real+fictitious to fictitious+real to fictitious) interpotentials. Since the first two interactions are equal, the interaction potential is calculated as the sum of the real-to-real charge interpotentials, plus one-half of the real-to-fictitious image charge interpotentials.

Extended dipole interactions

Self-image energy

A single molecule located β away from a metal feels an interaction with its self-image. Referring to Fig. 8, the potential energy for this interaction is

$$\Delta U(q)=\frac{q^2}{4\pi\epsilon_0}\left[+\frac{1}{2}\left[-\frac{1}{2\beta+d}-\frac{1}{2\beta-d}+\frac{1}{2\beta}+\frac{1}{2\beta}\right]\right]+\left[\frac{(\mu-\mu_0)^2}{8\pi\epsilon_0\alpha}\right], \tag{A3a}$$

$$U_{SE}\equiv\Delta U(q)=-\frac{\mu^2}{8\pi\epsilon_0}\left(\frac{1}{4\beta^3}\right)\left[\frac{1}{1-d^2/(2\beta)^2}\right]+\left[\frac{(\mu-\mu_0)^2}{8\pi\epsilon_0\alpha}\right]$$
$$=-\frac{1}{2}\mu^*\langle\mathbf{E}_{\text{image}}\rangle+\left[\frac{(\mu-\mu_0)^2}{8\pi\epsilon_0\alpha}\right], \tag{A3b}$$

$$\langle\mathbf{E}_{\text{image}}\rangle\equiv\frac{\mu}{16\pi\epsilon_0\beta^3}\left[\frac{1}{1-d^2/(2\beta)^2}\right]. \tag{A3c}$$

To find the equilibrium configuration, we again minimize $\Delta U(q)$ with respect to q, which at constant d, is the same as minimizing with respect to μ, to give the results for a single molecule adsorbed on a perfect metal

$$\frac{\partial(\Delta U(\mu))}{\partial\mu}=0\Rightarrow(\mu-\mu_0)$$
$$=\mu_0\frac{1}{\left[\left(\frac{4\beta^3}{\alpha}\right)\left(1-\left(\frac{d}{2\beta}\right)^2\right)-1\right]}$$
$$=(4\pi\epsilon_0\alpha)\langle\mathbf{E}_{\text{image}}\rangle, \tag{A4a}$$

$$\Delta U_{\min}=-\left(\frac{1}{2}\right)\langle\mathbf{E}_{\text{image}}\rangle\cdot\mu_0$$
$$=-\left[\frac{\mu_0^2}{8\pi\epsilon_0 4\beta^3}\right]\frac{1}{\left[1-\left(\frac{d_0}{2\beta}\right)^2-\frac{\alpha}{4\beta^3}\right]}. \tag{A4b}$$

This equation closely resembles the point dipole limit in Eq. (11).

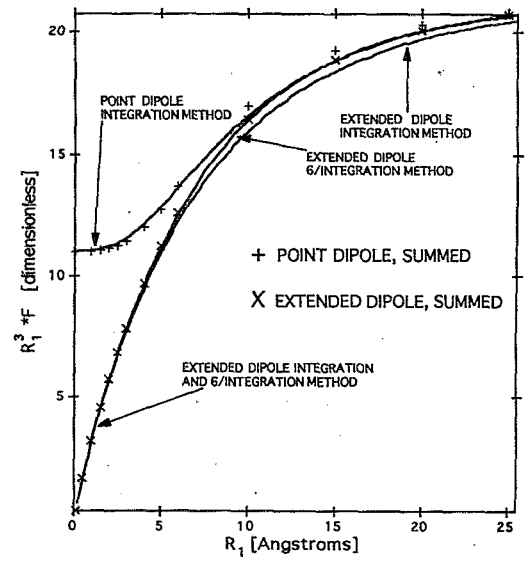

FIG. 9. Approximations for geometric dipole–dipole interaction term. Comparisons are made between values of the geometric factor $F(R_1)$ for point and extended dipoles, and for values obtained exactly (discrete summation) with those obtained using approximate methods. The ordinates of the plots are R_1, the nearest neighbor distance for adsorbates in a hexagonal lattice versus $R_1^3\cdot F(R_1)$. Large dipole charge separation distance ($d=4$ Å) is chosen to exaggerate differences between the approximations.

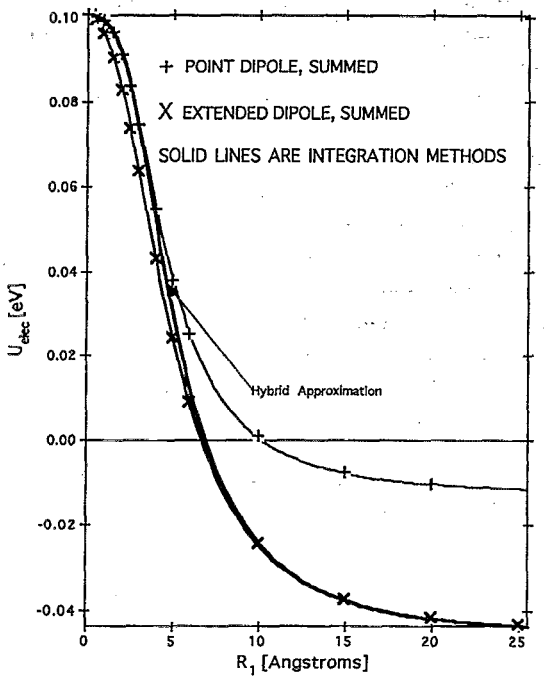

FIG. 10. Approximations for U_{elec}. The average binding energy is plotted versus nearest neighbor distance R_1 for the various approximations.

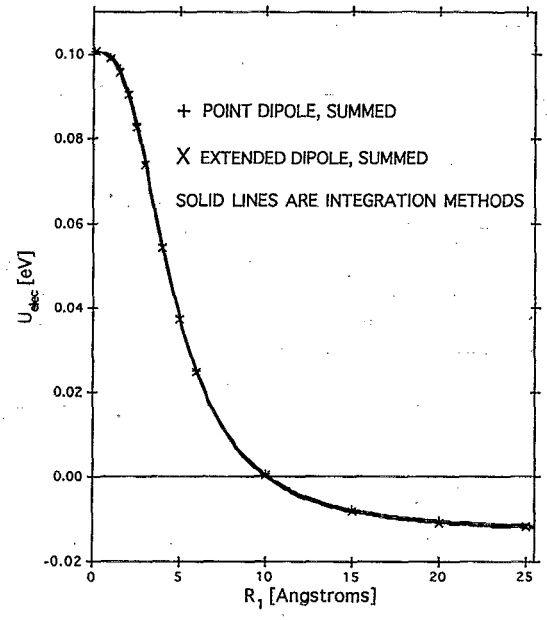

FIG. 11. Approximations for U_{elec} for dipole with more realistic charge separation distance ($d=1$ Å).

Energy of many dipoles

The energy of a hexagonal array of dipoles is calculated including the self-image energy of Eq. (A3), the lateral interactions, and the polarization potential energy (not yet minimized)

$$\Delta U(\mu)=-\frac{1}{2}\mu^*\langle \mathbf{E}_{\text{image}}\rangle+\left[\frac{(\mu-\mu_0)^2}{8\pi\epsilon_0\alpha}\right]+\frac{1}{2}\sum_j\left(\frac{q^2}{4\pi\epsilon_0}\right)\times\left[\left\{\frac{2}{R_j}-\frac{2}{\sqrt{R_j^2+d^2}}\right\}+\frac{1}{2}\left\{\frac{4}{\sqrt{R_j^2+(2\beta)^2}}-\frac{2}{\sqrt{R_j^2+(2\beta-d)^2}}-\frac{2}{\sqrt{R_j^2+(2\beta+d)^2}}\right\}\right],$$

$$=-\frac{1}{2}\mu^*\langle \mathbf{E}_{\text{image}}\rangle+\left[\frac{(\mu-\mu_0)^2}{8\pi\epsilon_0\alpha}\right]-\frac{1}{2}\mu^*\langle \mathbf{E}_d\rangle$$

$$=-\frac{1}{2}\mu^*\langle \mathbf{E}_t\rangle+\left[\frac{(\mu-\mu_0)^2}{8\pi\epsilon_0\alpha}\right], \tag{A5}$$

$$F_1(n)\equiv\sum_j\frac{1}{d^2}\left[\left\{\frac{2}{R_j}-\frac{2}{\sqrt{R_j^2+d^2}}\right\}+\frac{1}{2}\left\{\frac{4}{\sqrt{R_j^2+(2\beta)^2}}-\frac{2}{\sqrt{R_j^2+(2\beta-d)^2}}-\frac{2}{\sqrt{R_j^2+(2\beta+d)^2}}\right\}\right],$$

$$\langle \mathbf{E}_d\rangle\equiv-\left(\frac{\mu}{4\pi\epsilon_0}\right)F_1(n).$$

The factor of one half before the first summation in Eq. (A5) prevents double counting, the one-half inside the first summation properly treats image to real charge interactions. Note that in these equations the angle-bracketed average fields are substituted exactly, not approximately. (This is why this particular definition of the average field is so useful.) These equations closely parallel the equations for the point dipole case, with the term with most of the "extra algebra" contained in F_1. Minimizing the energy with respect to μ gives, as in Eqs. (16)–(17)

$$\left[\frac{(\mu-\mu_0)^2}{8\pi\epsilon_0\alpha}\right]=\frac{1}{2}\langle \mathbf{E}_t\rangle^*(\mu-\mu_0),$$

$$U_{\text{elec}}=-\frac{1}{2}\mu^*\langle \mathbf{E}_t\rangle+\frac{1}{2}\langle \mathbf{E}_t\rangle^*(\mu-\mu_0)$$

$$=-\frac{1}{2}\langle \mathbf{E}_t\rangle^*\mu_0, \tag{A6}$$

$$U_{\text{elec}}=\frac{\mu_0^2}{8\pi\epsilon_0}\frac{1}{\left(F_1(n)-\frac{1}{4\beta^3-\beta d^2}\right)^{-1}+\alpha}.$$

It is apparent that the extended dipole expressions can be obtained from the corresponding point dipole expressions by

replacing F with F_1, $4\beta^3$ with $4\beta^3-d^2\beta$, and replacing fields with our special average fields.

Comparison of point and extended dipoles, and their approximations

Evaluation of F_1 in Eq. (A5) can be accomplished by direct numerical summation. In Fig. 9 the extended dipole result for a specific set of parameters (α=7 Å^3, β=2.5 Å, μ_0=1.5 D, and d=4 Å) is compared with the point dipole limit with both summed numerically. The rather large value for d is chosen to examine the effect of various approximations. For large d, there is substantial difference between the extended and point dipole representations. Discrete summation to obtain F_1 is inconvenient compared to using an analytical expression. The summation of dipole terms has been treated many times (see Ref. 28, for example), but simple analytical results are often elusive. In the main text, an approximation was used to replace the discrete lattice for the point dipole with an integral. This same integration method can be applied here, (with $C=0.658$) and the results appear in Fig. 9. The integration methods for either the point or extended dipole case is within a few percent of giving the correct value for F_1.

At high dipole density, a discrete summation (e.g., Topping,[12] discussed in the main text) would be desirable, but is not applicable due to the square root terms of Eq. (A5). A mixed discrete summation and integral approximation provides an analytical alternative: We sum the contribution of the six nearest neighbors (for a hexagonal lattice) explicitly, then use an integral method for the remainder. We will term this method of approximation the 6/integration method. The integration is performed from a radius R_2 (which is adjusted to give the correct value of the integrals in the β=0 or ∞ limit) to infinity. The result is for a nearest neighbor spacing of $R_1=[1/n/\sin(60°)]^{0.5}$, with n the density of surface dipoles

$$F_1(n)\approx\frac{6}{d^2}\left[\left\{\frac{2}{R_1}-\frac{2}{\sqrt{R_1^2+d^2}}\right\}+\frac{1}{2}\left\{\frac{4}{\sqrt{R_1^2+(2\beta)^2}}-\frac{2}{\sqrt{R_1^2+(2\beta-d)^2}}-\frac{2}{\sqrt{R_1^2+(2\beta+d)^2}}\right\}\right]$$
$$+n\int_{R_2}^{\infty}dR\;R2\pi\,\frac{1}{d^2}\left[\frac{2}{R}-\frac{2}{\sqrt{R^2+d^2}}+\frac{2}{\sqrt{R^2+(2\beta)^2}}-\frac{1}{\sqrt{R^2+(2\beta-d)^2}}-\frac{1}{\sqrt{R^2+(2\beta+d)^2}}\right],\tag{A7}$$

$$=\frac{6}{d^2}\left[\frac{2}{R_1}-\frac{2}{\sqrt{R_1^2+d^2}}+\frac{2}{\sqrt{R_1^2+(2\beta)^2}}-\frac{1}{\sqrt{R_1^2+(2\beta-d)^2}}-\frac{1}{\sqrt{R_1^2+(2\beta+d)^2}}\right]$$
$$-\frac{n2\pi}{d^2}\left[2R_2-2\sqrt{R_2^2+d^2}+2\sqrt{R_2^2+(2\beta)^2}-\sqrt{R_2^2+(2\beta-d)^2}-\sqrt{R_2^2+(2\beta+d)^2}\right].$$

The limits of Eq. (A7) as β and d go to zero and as β goes to infinity and d goes to zero are

$$\lim_{\beta,d\to0}(F_1)\approx\left[\frac{1}{R_1^3}\right]\left(12+\left(\frac{R_1}{R_2}\right)\frac{8\pi}{\sqrt{3}}\right)\quad\text{with}\quad n=\frac{2}{\sqrt{3}R_1^2},\tag{A8}$$

$$\lim_{\beta\to\infty,d\to0}(F_1)\approx\left[\frac{1}{R_1^3}\right]\left(6+\left(\frac{R_1}{R_2}\right)\frac{4\pi}{\sqrt{3}}\right).$$

By setting $R_2=1.442R_1$ in Eq. (A8), we obtain the same limiting values as obtained by the Topping summation (22.06 and 11.03, respectively). The results obtained using this method are displayed in Fig. 9. Note that the 6/integration method is a fairly good approximation, deviating from the exact value of F_1 by less than 0.5%.

The effect of these approximations on the U_{elec} calculation is shown in Fig. 10. Note that at infinite density, U_{elec} in all cases converges to $(\mu_0)^2/(8\pi\epsilon_0\alpha)$. As the density increases, the molecules simply depolarize such that μ goes to zero, and the energy per molecule simply becomes the change in internal energy to change the polarization from μ_0 to 0.

The difference between the point and extended dipole calculation is large for U_{elec} in Fig. 10 while the two integration methods for the extended cases are barely distinguished from either each other or the discrete summation value. The difference between U_{elec} calculated from the point and extended dipole models is largest for *low* density, i.e., large R_1. Since in this limit the F's for point and extended models are the same (see Fig. 9), this difference in U_{elec} clearly comes from the self-image energy term. So perhaps we could spend less effort trying to get $F_1(n)$ perfectly. This suggests one final approximation. Using the simple point dipole integration for F [Eq. (34)], and inserting it into the energy expression for extended dipoles in Eq. (A6) (including the extended self-image energy term), one gets the "hybrid" approximation:

$$U_{\text{elec}} \approx \frac{\mu_0^2}{8\pi\epsilon_0} \frac{1}{\left(\frac{4\pi}{\sqrt{3}\cdot CR_s^3} \left(1 + \frac{1}{\left[1 + \left(\frac{2\beta}{CR_s} \right)^2 \right]^{3/2}} \right) - \frac{1}{4\beta^3 - \beta d^2} \right)^{-1} + \alpha}. \tag{A9}$$

The hybrid approximation is shown in Fig. 10. This hybrid method gives U_{elec} within a few percent of the exact summation method and with a much less algebra than the more accurate 6/integration method, over a wide range of density and even for d/β greater than 1.

Note that the large variances between the extended and point models are somewhat exaggerated by the large charge separation distance d. If d is decreased from 4 to 1 Å, the difference between F_1 for point and extended dipoles decreases to about half of that in Fig. 9. From the plots of U_{elec} shown in Fig. 11, it is clear that the simple point dipole integration approximation is adequate in this case.

Summary

In conclusion, we have derived formulae (similar to those presented in the main text for point dipoles) which describe extended dipole–dipole interactions near surfaces. We have quantitatively evaluated the differences between the different models (and various approximations thereof). We ascertain that if the distance d is less than ca. $\beta/2$, the differences between the extended and point dipole models on the binding energies is very small, making the simpler point dipole model preferred. When desired, the extended dipole model can be employed and very *accurately* (within 0.5%) represented using the 6/integration method [Eqs. (A7) and (A6)] (rather than a time-consuming summation). However, whenever an extended dipole treatment is warranted, the hybrid model [Eq. (A9)] provides a simpler expression, widely accurate to a few percent. In all cases, we provide simple, accurate, analytical expressions, providing an excellent alternative to awkward direct summation or restrictive approximations.

ACKNOWLEDGMENTS

This work was supported via the Office of Chemical Sciences, Division of Basic Energy Sciences, U.S. Department of Energy, and through financial assistance from Associated Western Universities. The authors also wish to thank S. E. Barlow, D. M. Friedrich, R. D. Knochenmuss, A. J. Peurrung, and G. K. Schenter for assistance in preparing this manuscript.

[1] C. Benndorf and T. E. Madey, Surf. Sci. **135**, 164 (1983).
[2] B. D. Kay, K. R. Lykke, J. R. Creighton, and S. J. Ward, J. Chem. Phys. **91**, 5120, 1989.
[3] A. Berko, W. Erley, and D. Sander, J. Chem. Phys. **93**, 8300 (1990).
[4] E. V. Albano, J. Chem. Phys. **85**, 1044 (1986).
[5] K. Klier, Y.-N. Wang, and G. W. Simmons, J. Phys. Chem. **97**, 633 (1993).
[6] L. W. Bruch, Surface Sci. **125**, 194 (1983).
[7] B. Boddenberg and R. Neipmann, Mol. Phys. **79**, 405 (1993).
[8] C. M. Mate, C.-T. Kao, and G. A. Somorjai, Surf. Sci. **206**, 145 (1988).
[9] G. D. Mahan and A. A. Lucas, J. Chem. Phys. **68**, 1344 (1978).
[10] M. Scheffler, Surf. Sci. **81**, 562 (1979).
[11] B. N. J. Persson and A. Liebsch, Surf. Sci. **110**, 356 (1981).
[12] J. Topping, Proc. R. Soc. London Ser. A **114**, 67 (1927).
[13] M. W. Roberts and C. S. McKee, *Chemistry of the Metal Gas Interface* (Clarendon, Oxford, 1978).
[14] E. V. Albano, Appl. Surf. Sci. **14**, 183 (1982–1983).
[15] E. V. Albano, J. M. Heras, P. Schrammen, M. Mann, and J. Holzl, Surf. Sci. **129**, 137 (1983).
[16] A. D. Buckingham, in *Intermolecular Forces*, Advances in Chemical Physics, Vol. 12, edited by J. O. Hirschfelder (Interscience, New York, 1967).
[17] E. A. Moelwyn-Hughes, *Physical Chemistry* (Pergamon, New York, 1961), pp. 308–310.
[18] H. Froehlich, *Theory of Dielectrics*, 2nd ed. (Clarendon, Oxford, 1958), p. 169.
[19] S. Holmstrom and S. Holloway, Surf. Sci. **173**, L647 (1986).
[20] N. D. Lang, S. Holloway, and J. K. Norskov, Surf. Sci. **150**, 24 (1985).
[21] A. Liebsch, Phys. Scripta **35**, 354 (1986).
[22] J. C. Maxwell, *A Treatise on Electricity and Magnetism* (Dover, New York, 1954), pp. 245–260.
[23] J. Applequist, J. R. Carl, and K.-K. Fung, J. Am. Chem. Soc. **94**, 2952 (1972).
[24] J. Applequist and C. E. Felder, J. Chem. Phys. **75**, 1863 (1981).
[25] P. R. Antoniewiez, Phys. Stat. B **86**, (1978) 645; W. C. Meixner and P. R. Antoniewiez, Phys. Rev. B **13**, 3276 (1976).
[26] H. Kreuzer and S. H. Payne, in *Dynamics of Gas-Surface Interactions*, edited by C. T. Rettner and M. N. R. Ashfold (Royal Society Chemistry, Cambridge, 1991); H. J. Kreuzer, Langmuir **8**, 774 (1992).
[27] D. H. Everett, Transact. Faraday Soc. **46**, 453 (1950).
[28] B. R. A. Nijboer and M. J. Renne, Chem. Phys. Lett. **2**, 35 (1969); M. J. Renne, Thesis, Univ. Utrecht (1971).